Experimental Critical Constants, Vapor Pressures, and Vapor and Liquid Densities for Pentafluoroethane (R-125)

ARTICLE *in* JOURNAL OF CHEMICAL & ENGINEERING DATA · JULY 1997

Impact Factor: 2.04 · DOI: 10.1021/je960362f

4 AUTHORS, INCLUDING:

Kenneth R. Hall
Texas A&M University
251 PUBLICATIONS **3,997** CITATIONS
SEE PROFILE

James C. Holste
Texas A&M University
132 PUBLICATIONS **1,306** CITATIONS
SEE PROFILE

Experimental Critical Constants, Vapor Pressures, and Vapor and Liquid Densities for Pentafluoroethane (R-125)

Horacio A. Duarte-Garza,† Carleton E. Stouffer, Kenneth R. Hall, and James C. Holste*

Department of Chemical Engineering, Texas A&M University, College Station, Texas 77843-3122

Kenneth N. Marsh‡ and Bruce E. Gammon

Thermodynamics Research Center, The Texas A&M University System, College Station, Texas 77843-3111

This paper presents measurements of vapor pressure from 220 K to 338 K, liquid density from 180 K to 350 K and up to 70 MPa and vapor density from 310 K to 480 K and up to 12 MPa for pentafluoroethane (R-125). Extrapolating the observed vapor pressures to the measured critical temperature (339.41 ± 0.01) K provides a critical pressure of (3.6391 ± 0.002) MPa. Using these values with the law of rectilinear diameters indicates a critical density of (4768 ± 7) mol·m^{-3}. Correlations provide values which agree with the measured values for the vapor densities within ± 0.05%, the liquid densities within ±0.1%, and the vapor pressures within ±0.05%. The results are compared with values from the literature.

Introduction

Fully halogenated chlorofluorocarbons (CFC) have been identified as a primary cause of the depletion of the stratospheric ozone layer. Because of their detrimental effect upon the environment, international agreements have restricted or terminated the production of CFC in the near future. This represents a major challenge to the refrigeration industry because several of these fluids are common working fluids for refrigeration equipment. A large scale application is in commercial freezers where the azeotrope R-502 has been the refrigerant of choice. One possible replacement for such applications which appears to have appropriate physical properties is pentafluoroethane (R-125) or mixtures containing R-125. This paper presents experimental *PVT* values which include vapor pressures, vapor densities and liquid densities (between 180 K and 480 K at pressures up to 70 MPa) and the critical temperature for R-125.

Experimental Section

The measurements included in this work are vapor pressures, the critical temperature, and vapor and liquid densities for R-125. A brief summary of each of the experimental methods used appears below; detailed descriptions of these apparatus appear elsewhere.

Materials. The samples of R-125 used for the measurements came from Allied Signal and E. I. du Pont Nemours & Co. The purity of the du Pont sample was reported by the manufacturer to be 99.2+ mol %, based upon gas chromatography measurements, with the most significant impurities shown as R-23 (trifluoromethane) at 0.34 mol % and R-218 (perfluoroethane) at 0.16 mol %. The Allied Signal sample came from a lot specially prepared for research purposes. The supplier provided the following statement with the sample: "Our analysis shows a purity of 99.999+ area % by GC with FID. Further GC mass spec. could not identify any impurities. The moisture in this sample was measured as 2 ppm by wt." We did not perform a separate analysis on our sample, but a similar sample used by NIST was tested by Bruno (1994) and found to be free of other refrigerant impurities. The Allied Signal sample was used to measure the vapor pressures, critical point, and most of the liquid densities. The du Pont sample was used for some of the liquid density measurements and for the superheated vapor phase measurements where impurity effects were less important. A comparison of liquid density results for the different samples confirmed agreement within the accuracy of the experiment, and an error analysis of the vapor phase measurements indicated that the impurities did not affect the results significantly. Three freeze/thaw cycles were employed attempting to remove the dissolved air from the samples.

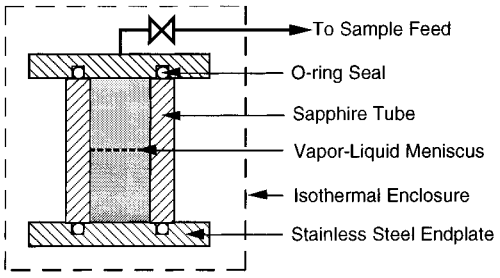

Figure 1. Schematic of critical point apparatus.

Vapor Pressure Measurements. The vapor pressure measurements utilize an isochoric apparatus. Yurttas *et al.* (1994) provide a detailed description of this apparatus which consists of a sample cell surrounded by an isothermal vessel. Temperatures are measured with a MINCO platinum resistance thermometer with a precision of ± 0.001 K and an accuracy of ±0.01 K on IPTS-68. Temperatures have been converted to ITS-90. Pressures are measured with a DH Instruments Model 26000 automatic pressure standard (dead weight gauge) certified accurate to ±0.005% combined with a differential pressure indicator of our own design which is an integral part of the isochoric cell. The differential pressure indicator has an accuracy of ±200 Pa. Sample loading into the cell occurs at an overall density slightly higher than the critical density to avoid errors caused by adsorption of sample on the cell wall. The estimated accuracy of the vapor pressure measurements is the greater of ±0.05% or ±200 Pa (assuming a pure sample).

* Corresponding author.
† Current address: Texas A&M University−Kingsville, Kingsville, TX 78363.
‡ Current address: University of Canterbury, Private Bag 4800, Christchurch, New Zealand.

S0021-9568(96)00362-7 CCC: $14.00

Critical Temperature Measurement. The cylindrical sapphire cell shown in Figure 1, which has an internal volume of about 4 cm^3, was used to determine the critical temperature of R-125 by observing visually the appearance or disappearance of the meniscus. The cell was immersed in a well-stirred bath where the temperature was measured and controlled to within ±0.001 K. A Rosemount platinum resistance thermometer, located adjacent to the sample cell, provided the temperature with a precision of ±0.001 K and an accuracy of ±0.01 K on IPTS-68 (subsequently converted to ITS-90). The initial measurements established the critical temperature within ±0.050 K. This value was improved by observing the state of the meniscus following increasing temperature increments of 0.010 K until the meniscus disappeared. The state of the meniscus was observed 24 h after each 0.010 K increment in temperature because we observed that often the meniscus appeared or disappeared as much as 8 h after a temperature change. This procedure was repeated for decreasing temperature increments to observe the appearance of the meniscus. Thus the observed value for the critical temperature should be accurate within ±0.010 K.

The critical temperature uncertainty includes that associated with observing the meniscus disappearance. The critical pressure results from extrapolating the vapor pressure measurements to the observed critical temperature. The critical density involves extrapolating the saturated vapor and liquid densities using the law of rectilinear diameters.

Vapor Density Measurement. A Burnett apparatus and an isochoric apparatus provide the vapor density measurements. The isochoric apparatus is the same as that used for the vapor pressure measurements, while Stouffer (1992) describes the Burnett apparatus. It consists of two cylindrical, stainless steel cells with polished interiors housed in an aluminum enclosure insulated by vacuum and controlled to provide an isothermal environment. The essence of the experiment is to expand repeatedly the fluid sample from one volume into a second, evacuated volume. The temperature and pressure are measured after each expansion. The densities before and after the expansions are related by the geometry of the apparatus, *i.e.*, the ratio of the volume of the first cell to the total volume of the two cells. The sequence of expansions during the Burnett experiment produces a series of pressures related by a constant ratio of densities. A nonlinear, statistical analysis utilizing the virial equation of state then provides the densities and virial coefficients without requiring direct measurement of the mass or total volume. The methods for measuring the pressure and temperature and measurement accuracies are similar to those described for the isochoric apparatus. The estimated accuracy of the vapor densities varies between ±0.02% and ±0.04% from the lowest to the highest pressure.

Liquid Density Measurements. The liquid density measurements utilize a continuously weighed pycnometer described by Lau (1986). It consists of a sample cell suspended from an electronic balance and surrounded by an isothermal helium bath and copper shield. The mass of the sample cell comes from weighing, while the volume of the cell results from calibration at several temperatures and pressures with degassed, deionized liquid water. The electronic balance (Arbor Model 507) has a capacity of 0.5 kg and a resolution of 0.1 mg. The sample cell volume is approximately 10 cm^3. The pressure of the sample is measured with a strain gauge pressure transducer (Rosemount, Model 1333G10) with an accuracy of ±0.01 MPa. The temperature of the sample cell is measured with a MINCO platinum resistance thermometer (Model S-1069). The temperature measurements are precise to ±0.001 K and accurate to ±0.01 K after conversion from IPTS-68 to ITS-90. The liquid densities are accurate within ±0.1%.

Results

The measurements of this work include vapor pressures, compressed liquid densities, the critical temperature, and vapor densities of R-125. The distribution of the measurements as a function of temperature and pressure constitutes Figure 2.

Vapor Pressures. Vapor pressure measurements range from 220 K to 338.5 K. The vapor pressure measurements have been correlated with the equation proposed by Iglesias-Silva *et al.* (1987)

$$p(t) = [p_0(t)^N + p_\infty(t)^N]^{1/N} \tag{1}$$

where

$$p(t) = 1 + (P - P_t)/(P_c - P_t)$$

$$t = (T - T_t)/(T_c - T_t)$$

$$p_0(t) = a_0 + a_1(a_3 t + 1)^{b_0/R} \exp[(-a_2 + b_0/R)/(a_3 t + 1)]$$

$$p_\infty(t) = 2 - a_4(1 - t) + a_5(1 - t)^{2-\theta} + a_6(1 - t)^3 + a_7(1 - t)^4$$

$$a_0 = 1 - P_t/(P_c - P_t)$$

$$a_1 = (1 - a_0) \exp(a_2 - b_0/R)$$

$$a_2 = b_1/RT_t$$

$$a_3 = (T_c - T_t)/T_t$$

$$a_5 = -0.115\,991\,04 + 0.295\,062\,58a_4^2 - 0.000\,212\,22a_4^5$$

$$a_6 = -0.015\,460\,28 + 0.089\,781\,6a_4^2 - 0.053\,221\,99a_4^3$$

$$a_7 = 0.057\,257\,57 - 0.068\,176\,87a_4 + 0.000\,471\,88a_4^5$$

$$N = 87T_t/T_c$$

$$\theta = 0.2$$

where T_t is the triple point temperature, T_c is the critical temperature, P_t is the triple point pressure, and P_c is the critical pressure.

The experimental vapor pressures appear in Table 1. The parameters that give the best fit of eq 1 are given in Table 2. Figure 3 shows the deviations from eq 1 of the present results along with values reported in the literature by other workers.

Critical Temperature. The measured critical temperature of R-125 was (339.410 ± 0.010) K by direct observation of the disappearance and reappearance of the vapor−liquid interface. The critical pressure, (3.6391 ± 0.0002) MPa, resulted from extrapolating the vapor pressure curve developed in this work to the measured critical temperature. The critical density, (4768 ± 7) $mol \cdot m^{-3}$, resulted from extrapolating the saturated vapor and liquid densities to the critical temperature using the law of rectilinear diameters.

Vapor Densities. The vapor density measurements consist of two replications each of Burnett isotherms at

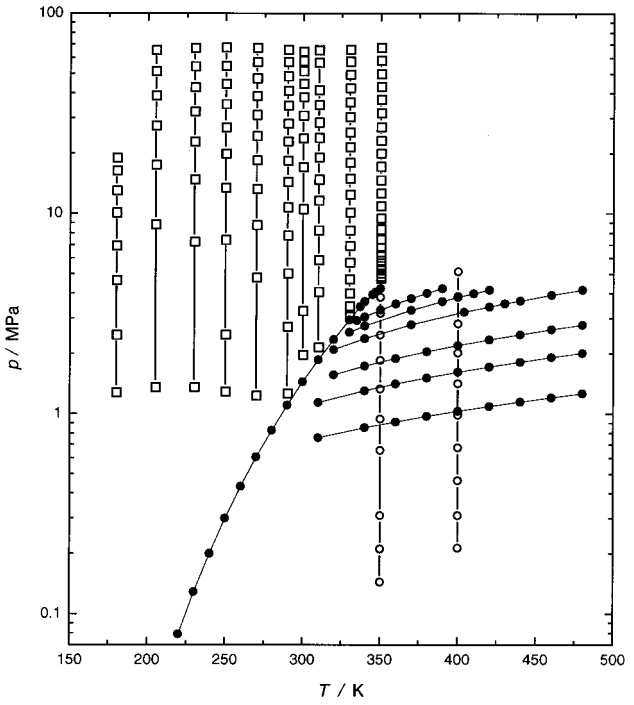

Figure 2. Distribution of *PVT* and vapor pressure measurements for R-125 . The symbols denote: ●, vapor pressure and isochoric measurements; ○, Burnett measurements; □, continuously weighed pycnometer measurements.

Table 1. Vapor Pressure Measurements for R-125

T/K	*P*/kPa	P_{calc}/kPa	$100(P - P_{calc})/P$
220.004	79.23	79.27	−0.050
230.000	128.94	128.85	0.070
239.998	200.31	200.35	−0.021
249.999	299.97	299.75	0.073
260.001	433.25	433.36	−0.026
290.000	1106.04	1106.39	−0.032
299.998	1447.57	1447.28	0.020
309.999	1862.55	1862.29	0.014
319.997	2362.39	2362.43	−0.002
329.999	2961.95	2962.17	−0.007
331.998	3095.43	3095.69	−0.009
333.997	3234.34	3234.34	−0.000
335.999	3378.63	3378.72	−0.003
336.997	3453.02	3452.94	0.002
337.999	3529.18	3529.10	0.002

Table 2. Parameters for Equation 1 for the Vapor Pressure of R-125[a]

$a_4 = 3.736\ 171$
$b_0 = -36.049\ 408\ \text{J·mol}^{-1}\text{·K}^{-1}$
$b_1 = 22\ 105.014\ 689\ \text{J·mol}^{-1}$
$T_t = 170.0\ \text{K}$
$P_t = 2.565\ \text{kPa}$
$T_c = 339.410\ \text{K}$
$P_c = 3639.1\ \text{kPa}$
$R = 8.314\ 48\ \text{J·mol}^{-1}\text{·K}^{-1}$

[a] T_t and P_t have been adjusted slightly from the values reported by Iglesias-Silva *et al.* (1995) to achieve a better fit.

350.0 K and at 400.0 K and seven isochores at temperatures ranging from 310.0 K to 480.0 K up to 4 MPa. The Burnett measurements are in Table 3 and the isochoric measurements are in Table 4. At 350 K and 400.0 K, the second virial coefficients, *B*, for R-125 are respectively (-2.478×10^{-4} and -1.727×10^{-4}) $\text{m}^3\text{·mol}^{-1}$; the third virial coefficients are respectively (2.333×10^{-8} and 1.675×10^{-8}) $\text{m}^6\text{·mol}^{-2}$. These virial coefficients compare to those of Boyes and Weber (1995) at 350 K, $B = -2.482 \times 10^{-4}\ \text{m}^3\text{·mol}^{-1}$ and $C = 2.3541 \times 10^{-8}\ \text{m}^6\text{·mol}^{-2}$, and to

Table 3. Burnett Isotherms for R-125

T/K	*P*/MPa	ρ/mol·m^{-3}	*Z*
	350 K: Isotherm 1		
350.000	6.353 813	8030.5	0.271 89
350.000	4.615 296	5435.1	0.291 80
349.993	4.274 686	3678.5	0.399 34
349.998	3.823 185	2489.6	0.527 71
350.012	3.181 706	1684.97	0.648 86
350.000	2.481 779	1140.40	0.747 83
349.996	1.847 886	771.82	0.822 73
349.996	1.333 240	522.37	0.877 06
350.002	0.941 893	353.54	0.915 49
349.998	0.656 113	239.28	0.942 26
349.997	0.452 764	161.946	0.960 73
350.000	0.310 354	109.605	0.973 02
350.002	0.211 686	74.181	0.980 60
349.994	0.144 019	50.206	0.985 75
	350 K: Isotherm 2		
349.997	5.562 216	7431.9	0.257 19
349.994	4.537 092	5030.0	0.309 97
349.998	4.204 211	3404.3	0.424 38
349.994	3.706 630	2304.0	0.552 83
349.984	3.041 136	1559.38	0.670 19
349.997	2.347 519	1055.40	0.764 35
349.989	1.735 270	714.30	0.834 83
349.994	1.245 887	483.44	0.885 61
349.989	0.877 460	327.19	0.921 58
349.996	0.609 912	221.45	0.946 46
350.001	0.420242	149.875	0.963 53
	400 K: Isotherm 1		
400.000	12.044 877	6426.72	0.563 53
399.997	8.093 511	4346.37	0.559 91
400.003	6.230 916	2939.43	0.637 37
399.999	4.782 627	1987.93	0.723 37
399.997	3.568 101	1344.48	0.797 80
399.997	2.589 756	909.287	0.856 34
399.998	1.839 762	614.960	0.899 68
399.999	1.287 182	415.901	0.930 71
399.996	0.890 518	281.276	0.952 48
399.999	0.611 806	190.227	0.967 56
400.004	0.418 195	128.651	0.977 92
399.994	0.284 933	87.0063	0.985 00
399.998	0.193 708	58.8422	0.989 83
	400 K: Isotherm 2		
399.998	14.446 066	7132.61	0.608 99
400.001	8.746 958	4823.76	0.545 22
399.995	6.651 912	3262.30	0.613 10
399.999	5.137 173	2206.28	0.700 11
400.000	3.866 949	1492.10	0.779 45
399.998	2.826 770	1009.13	0.842 33
399.996	2.019 241	682.484	0.889 47
400.000	1.417 708	461.569	0.923 47
399.997	0.983 858	312.161	0.947 43
399.997	0.677 175	211.115	0.964 07
399.999	0.463 462	142.777	0.975 53
399.998	0.315 992	96.5601	0.983 37
399.998	0.214 934	65.3034	0.988 72

those of Gillis (1997) at 350 K, $B = -2.474 \times 10^{-4}\ \text{m}^3\text{·mol}^{-1}$, and at 400 K, $B = -1.739 \times 10^{-4}\ \text{m}^3\text{·mol}^{-1}$ and $C = 1.67 \times 10^{-8}\ \text{m}^6\text{·mol}^{-2}$. The isochoric vapor densities have been calculated from the isochoric measurements using densities derived from the 400.0 K Burnett measurements. For a given isochore, the densities along the isochore have been corrected to account for the distortion of the sample cell volume with temperature and pressure. For the pressure range studied, the pressure distortion correction is negligible and the temperature distortion correction is

$$\rho/\rho(400\ \text{K}) = [1.0 - \alpha(400.0 - T/\text{K})]^{-1} \qquad (2)$$

where α is the coefficient of thermal expansion for Type 316 stainless steel ($4.8 \times 10^{-5}\ \text{K}^{-1}$), *T* is the temperature,

Table 4. Isochoric Temperatures and Pressures (Measured) and Densities (Derived) for R-125 Vapor

T/K	P/MPa	ρ/mol·m^{-3}	ρ_{calc}/mol·m^{-3}	$100(\rho - \rho_{calc})/\rho$
		Isochore 1		
339.996	3.646 126	3427.2	3411.1	0.4707
344.996	3.945 027	3425.5	3429.3	−0.1110
347.000	4.062 127	3424.7	3430.8	−0.1770
349.998	4.235 337	3424.2	3432.9	−0.2539
		Isochore 2		
335.000	2.934 405	1810.1	1808.2	0.1041
340.000	3.060 715	1809.7	1808.3	0.0784
350.000	3.306 116	1808.8	1806.9	0.1077
360.000	3.544 416	1807.9	1805.5	0.1347
370.000	3.777 227	1807.1	1804.5	0.1440
380.000	4.005 517	1806.2	1803.8	0.1317
390.000	4.230 227	1805.3	1803.4	0.1042
		Isochore 3		
419.996	4.158 247	1468.6	1468.6	−0.0580
410.000	3.991 427	1468.8	1469.3	−0.0588
399.996	3.822 837	1469.1	1470.0	−0.0618
389.994	3.651 876	1469.9	1470.5	−0.0514
370.000	3.302 576	1471.2	1471.6	−0.0283
340.000	2.753 555	1473.3	1474.3	−0.0655
330.000	2.560 045	1474.0	1474.2	−0.0126
		Isochore 4		
479.993	4.163 607	1159.4	1159.1	0.0276
459.993	3.922 687	1160.6	1160.5	0.0090
439.994	3.679 186	1161.7	1161.8	−0.0122
430.000	3.556 116	1162.2	1162.4	−0.0193
419.995	3.431 876	1162.8	1163.0	−0.0136
400.000	3.180 68	1163.9	1164.2	−0.0261
369.995	2.792 605	1165.6	1166.1	−0.0456
340.000	2.385 344	1167.3	1168.2	−0.0762
320.000	2.095 984	1168.4	1167.3	0.0942
		Isochore 5		
479.992	2.785 065	749.0	749.0	−0.0032
460.000	2.640 865	749.8	749.6	0.0256
439.994	2.495 514	750.5	750.3	0.0248
420.000	2.348 774	751.2	751.1	0.0093
400.000	2.199 694	751.9	751.9	−0.0028
379.994	2.048 004	752.6	752.8	−0.0233
359.997	1.893 223	753.4	753.7	−0.0432
340.000	1.734 303	754.1	754.7	−0.0806
320.004	1.569 373	754.8	755.2	−0.0501
		Isochore 6		
479.999	2.012 864	530.6	530.8	−0.0384
459.996	1.914 913	531.2	531.1	0.0137
439.998	1.816 473	531.7	531.6	0.0279
420.001	1.717 343	532.2	532.1	0.0215
399.997	1.617 043	532.7	532.7	0.0074
379.999	1.515 363	533.2	533.3	−0.0122
360.000	1.412 002	533.7	533.9	−0.0398
339.996	1.306 492	534.2	534.6	−0.0692
309.999	1.142 292	535.0	535.0	0.0000
		Isochore 7		
479.996	1.265 022	327.1	327.3	−0.0600
459.997	1.206 982	327.5	327.4	0.0236
440.001	1.149 022	327.8	327.7	0.0375
419.999	1.090 882	328.1	328.0	0.0230
399.998	1.032 222	328.4	328.4	0.0052
379.997	0.972 692	328.7	328.7	0.0133
359.993	0.912 712	329.0	329.0	−0.0085
339.997	0.851 902	329.3	329.4	−0.0293
310.000	0.758 351	329.8	329.7	0.0164

ρ is the density at temperature T, and ρ(400 K) is the density at 400 K.

The vapor densities for temperatures between 390 K and 480.0 K have been correlated using a truncated virial equation of state

$$Z = \frac{P}{\rho RT} = 1 + B\rho + C\rho^2 \qquad (3)$$

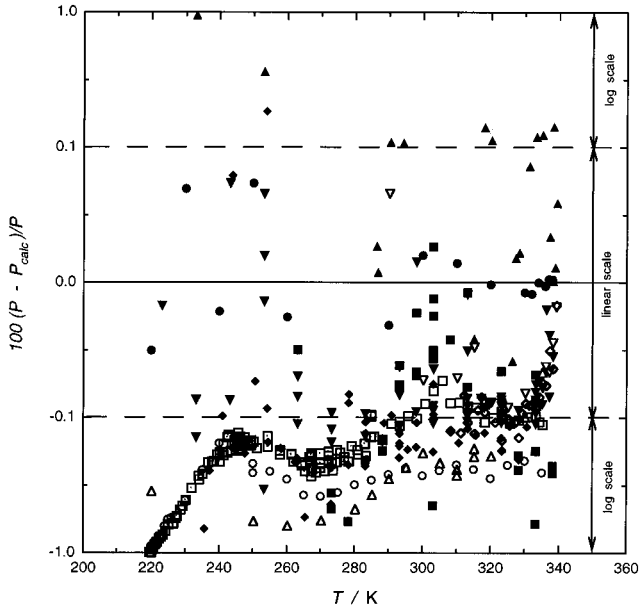

Figure 3. Deviations of experimental vapor pressures for R-125 from values calculated using eq 1 and the parameters listed in Table 2. The symbols denote ●, this work; ▼, Oguchi *et al.* (1996); ▽, Ye *et al.* (1995); ■, Tsvetkov *et al.* (1995); □, Weber and Silva (1994); △, Widiatmo *et al.* (1994); □, Boyes and Weber (1995); ◆, Sagawa *et al.* (1994); ◇, Baroncini *et al.* (1993); ○, Magee (1996); ▲, Singh (1994). The plot utilizes the technique proposed by Holste *et al.* (1996) for the ordinate.

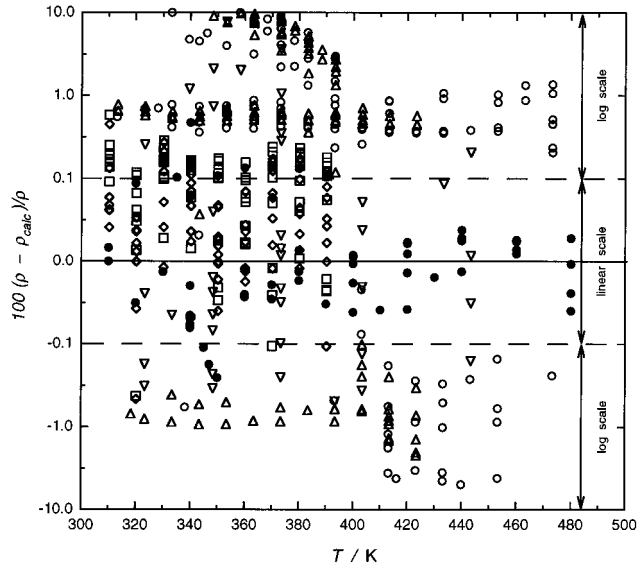

Figure 4. Deviations of the measured superheated vapor densities for R-125 from values calculated using eq 3 using the parameters listed in Table 5. The symbols denote: ●, this work; ▽, Tsvetkov *et al.* (1995); ○, Oguchi *et al.* (1996); △, Sagawa *et al.* (1994); ◇, Ye *et al.* (1995); □, Zhang *et al.* (1996). The plot utilizes the technique proposed by Holste *et al.* (1996) for the ordinate.

where

$$B = b_0 + \frac{b_1}{T^{1/2}} + \frac{b_2}{T} + \frac{b_3}{T^2}$$

$$C = c_0 + \frac{c_1}{T^{1/2}} + \frac{c_2}{T} + \frac{c_3}{T^2}$$

Z is the compressibility factor, P is the pressure, R is the gas constant, T is the temperature, and B and C are the second and third virial coefficients respectively, with b_i and

Table 5. Parameters for Equation 3 for the Vapor Density of R-125

b_0	$-3.528\ 89 \times 10^{-4}$ m^3·mol^{-1}
b_1	$1.972\ 686 \times 10^{-2}$ m^3·K$^{0.5}$·mol^{-1}
b_2	$-0.254\ 077$ m^3·K·mol^{l-1}
b_3	-27.3083 m^3·K^2·mol^{-1}
c_0	$1.569\ 744 \times 10^{-6}$ m^6·mol^{-2}
c_1	$-8.184\ 63 \times 10^{-5}$ m^6·K$^{0.5}$·mol^{-2}
c_2	$1.195\ 3541 \times 10^{-3}$ m^6·K·mol^{-2}
c_3	$-0.071\ 909$ m^6·K^2·mol^{-2}

c_i being the parameters of the fit. The values of the parameters which give the best fit of eq 3 to the vapor densities of R-125 are in Table 5. Figure 4 shows the deviations of the vapor density measurements from eq 3.

Liquid Densities. The liquid densities for R-125 at temperatures ranging from 180 K to 350 K at pressures from slightly above the vapor pressure up to about 70 MPa appear in Table 6. At 180 K, the sample solidifies at about 20 MPa. The 151 measured liquid densities have been correlated using a modified Benedict−Webb−Rubin equation

$$\frac{P}{\rho RT} - 1.0 = \sum_{n=1}^{8} a_n \rho_r^n + \exp(-\rho_r^2) \sum_{n=9}^{14} a_n \rho_r^{2n-16} \qquad (4)$$

where the coefficients are functions of temperature

$$a_1 = b_1 + b_2 T_r^{-0.5} + b_3 T + b_4 T_r^{-2} + b_5 T_r^{-3}$$

$$a_2 = b_6 + b_7 T_r^{-1} + b_8 T_r^{-2} + b_9 T_r^{-3}$$

$$a_3 = b_{10} + b_{11} T_r^{-1} + b_{12} T_r^{-2}$$

$$a_4 = b_{13} T_r^{-1}$$

$$a_5 = b_{14} T_r^{-2} + b_{15} T_r^{-3}$$

$$a_6 = b_{16} T_r^{-2}$$

$$a_7 = b_{17} T_r^{-2} + b_{18} T_r^{-3}$$

$$a_8 = b_{19} T_r^{-3}$$

$$a_9 = b_{20} T_r^{-3} + b_{21} T_r^{-4}$$

$$a_{10} = b_{22} T_r^{-3} + b_{23} T_r^{-5}$$

$$a_{11} = b_{24} T_r^{-3} + b_{25} T_r^{-5}$$

$$a_{12} = b_{26} T_r^{-3} + b_{27} T_r^{-5}$$

$$a_{13} = b_{28} T_r^{-3} + b_{29} T_r^{-4}$$

$$a_{14} = b_{30} T_r^{-3} + b_{31} T_r^{-4} + b_{32} T_r^{-5}$$

and T_r is T/T_c, $T_c = 339.41$ K, ρ_r is ρ/ρ_c, and ρ_c is 4768 mol·m^{-3}. The fit parameters of eq 4 which describe the experimental liquid densities of R-125 within ±0.1% appear in Table 7. The values of the vapor densities calculated from this equation agree with the experimental values within ±0.05%. Figure 5 shows the deviations of the liquid density measurements from eq 4.

Discussion

Vapor Pressures. Figure 3 shows the deviations of our experimental values and literature values from eq 1 (which has been fit using only the current measurements). The estimated uncertainty of our vapor pressure measurements is ±0.05% at temperatures above 290 K with the largest uncertainty of ±0.3% at 220 K. The measurements by Oguchi *et al.* (1996) agree with our values within ±0.2% over the entire temperature range. Their estimated uncertainty is about ±0.6% in the temperature range 220 K to 260 K and ±0.3% from 260 K to 339 K. The measurements of Ye *et al.* (1995) agree with our data within ±0.06%. The estimated uncertainty of their vapor pressure values is ±0.15%. Our values agree with those of Tsvetkov *et al.* (1995) within ±0.2%, which is their estimated uncertainty. Our vapor pressure values are slightly higher than those of Boyes and Weber (1995) and Magee (1996), but the three sets agree within ±0.2% (our estimated uncertainty over the temperature range 275 K to 339 K is ±0.05% as is theirs, both assuming pure sample). Our vapor pressures are 0.2% to 0.6% higher than those of Widiatmo *et al.* (1994), whose estimated uncertainty is ±0.2%. Our results deviate from those of Weber and Silva (1994) by as much as ±1.0% at temperatures below 240 K and by about ±0.2% at temperatures above 240 K. Their estimated uncertainty is less than ±0.05% over the entire temperature range. Measurements by Sagawa *et al.* (1994) agree with our values within ±0.15%, which corresponds to their estimated uncertainty. Most of the values reported by Baroncini *et al.* (1993) agree with our values within ± 0.2%, which again is their estimated uncertainty. The measurements of Monluc *et al.* (1991) agree with our measurements within ±0.15% while their estimated uncertainty is ±0.2%. These deviations do not appear in Figure 3. Singh (1994) measured the vapor pressure of a sample produced in the same batch as ours. His values are about 0.07% higher than ours. Given that our results are about 0.1% higher than the majority of reported values, it is conceivable that our sample was contaminated by a small amount of volatile impurity such as air or helium during the loading process, but Singh (1994) would also then have approximately the same amount of volatile impurity introduced into his sample. The samples used by most of the other investigations contain R-115 as a contaminant which would cause their measurements to be low. While the investigators attempted to correct for this effect, it is also conceivable that some of the effect remains.

Wilson *et al.* (1992) have published a correlation based upon their measurements for the vapor pressure of R-125 from 195.0 K to the critical temperature. Because they do not report their experimental values, they cannot be compared to ours, but they report an average absolute deviation between their measured vapor pressures and values calculated from their correlation of ±0.25% with a maximum deviation of ±1.3%.

Vapor Densities. Figure 4 shows the deviation from eq 3 of our measured vapor densities and those of Tsvetkov *et al.* (1995), Baroncini *et al.* (1993), Oguchi *et al.* (1996), Sagawa *et al.* (1994), Ye *et al.* (1995), and Zhang *et al.* (1996). Wilson *et al.* (1992) present vapor densities over a temperature range from 195 K to 450 K along with a correlation which reproduces their results within ±1%, but these results have not been included in the figure because of the narrow region of overlap.

For adsorbing fluids, significant inaccuracies in vapor density measurements may result from adsorption effects

Table 6. Pycnometric Measurements of Liquid Densities for R-125[a]

T/K	P/MPa	ρ_{exp}/mol·m^{-3}	ρ_{cal}/mol·m^{-3}	% dev	T/K	P/MPa	ρ_{exp}/mol·m^{-3}	ρ_{cal}/mol·m^{-3}	% dev
180.000	19.0497	14 152.9	14 152.3	0.005	180.000	6.9596	13 992.2	13 991.7	0.004
180.000	16.4838	14 119.8	14 119.5	0.002	180.000	4.6819	13 958.9	13 959.5	−0.005
180.000	13.0966	14 075.8	14 075.2	0.005	180.000	2.4942	13 927.5	13 928.0	−0.004
180.000	10.1578	14 036.7	14 035.7	0.007	180.000	1.2898	13 908.7	13 910.4	−0.012
205.000	65.8285	14 158.9	14 161.1	−0.015	205.000	17.5843	13 522.8	13 524.2	−0.010
205.000	51.7934	14 000.9	14 000.9	0.000	205.000	8.8870	13 372.6	13 373.7	−0.008
205.000	38.9736	13 839.3	13 839.0	0.002	205.000	1.3673	13 227.4	13 228.7	−0.010
205.000	27.6557	13 680.5	13 680.7	−0.001					
230.000	67.5358	13 697.1	13 695.3	0.013	230.000	22.9295	13 012.4	13 009.6	0.022
230.000	54.8481	13 531.9	13 529.1	0.020	230.000	14.8669	12 846.4	12 842.2	0.032
230.000	42.9669	13 359.2	13 356.0	0.024	230.000	7.2919	12 668.4	12 663.0	0.042
230.000	32.4505	13 186.4	13 184.4	0.015	230.000	1.3720	12 510.4	12 502.3	0.065
250.000	67.7798	13 311.1	13 316.7	−0.042	250.000	1.2975	11 863.4	11 864.2	−0.007
250.000	54.9040	13 120.0	13 126.4	−0.049	250.000	67.3366	13 317.4	13 310.5	0.052
250.000	44.7122	12 951.7	12 957.7	−0.047	250.000	52.2951	13 090.3	13 085.0	0.041
250.000	35.4535	12 777.8	12 786.5	−0.069	250.000	39.5909	12 869.1	12 865.5	0.028
250.000	27.1043	12 606.4	12 613.0	−0.053	250.000	27.9594	12 634.5	12 631.8	0.021
250.000	20.0319	12 438.8	12 447.3	−0.068	250.000	18.3935	12 408.0	12 405.8	0.017
250.000	13.5524	12 269.5	12 275.1	−0.045	250.000	10.0476	12 175.0	12 171.3	0.030
250.000	7.4493	12 082.9	12 088.2	−0.044	250.000	5.5224	12 027.4	12 022.7	0.039
250.000	2.4978	11 910.3	11 911.6	−0.011	250.000	1.3564	11 871.1	11 866.6	0.039
270.000	67.5786	12 937.6	12 937.7	−0.001	270.000	18.5660	11 874.0	11 880.6	−0.055
270.000	57.4266	12 768.6	12 770.6	−0.015	270.000	13.3732	11 698.9	11 703.8	−0.042
270.000	47.6582	12 588.7	12 591.5	−0.022	270.000	8.8055	11 522.8	11 524.6	−0.015
270.000	38.9281	12 407.7	12 411.9	−0.034	270.000	4.8224	11 343.8	11 342.3	0.013
270.000	31.2426	12 228.6	12 233.8	−0.043	270.000	1.2415	11 151.4	11 147.9	0.031
270.000	24.4974	12 050.8	12 057.1	−0.053					
290.000	66.2920	12 544.0	12 546.0	−0.016	290.000	18.4676	11 319.9	11 325.2	−0.047
290.000	57.5571	12 380.2	12 383.4	−0.026	290.000	14.4676	11 149.4	11 154.2	−0.043
290.000	48.8664	12 199.8	12 203.7	−0.032	290.000	10.7979	10 970.1	10 974.1	−0.036
290.000	41.3978	12 025.9	12 031.1	−0.043	290.000	7.8473	10 803.3	10 806.7	−0.032
290.000	34.8216	11 855.6	11 861.2	−0.047	290.000	5.0718	10 621.7	10 623.1	−0.013
290.000	28.3085	11 664.9	11 671.3	−0.055	290.000	2.7440	10 438.7	10 440.2	−0.015
290.000	23.0354	11 490.8	11 496.7	−0.051	290.000	1.2741	10 305.1	10 304.5	0.006
300.000	56.0143	12 165.3	12 158.7	0.055	300.000	12.3362	10 739.8	10 729.3	0.098
300.000	45.7916	11 934.3	11 926.1	0.069	300.000	8.7202	10 510.4	10 501.6	0.084
300.000	37.6842	11 719.6	11 713.6	0.051	300.000	5.7554	10 279.6	10 274.0	0.055
300.000	29.5628	11 472.9	11 466.1	0.059	300.000	3.1145	10 025.7	10 019.0	0.067
300.000	23.3498	11 245.9	11 243.6	0.020	300.000	1.7785	9 861.6	9 858.2	0.035
300.000	18.0901	11 024.7	11 022.7	0.018	300.000	65.1245	12 343.5	12 341.3	0.018
300.000	13.3784	10 788.8	10 787.7	0.010	300.000	55.1812	12 141.4	12 140.9	0.004
300.000	9.7116	10 569.1	10 568.5	0.006	300.000	44.5333	11 895.2	11 894.9	0.002
300.000	6.2950	10 318.5	10 319.1	−0.006	300.000	35.6664	11 658.1	11 655.9	0.019
300.000	3.6831	10 079.5	10 079.7	−0.002	300.000	28.5261	11 432.1	11 431.3	0.007
300.000	1.8000	9 860.0	9 861.0	−0.010	300.000	21.9576	11 189.3	11 188.5	0.007
300.000	54.9117	12 147.8	12 135.1	0.104	300.000	16.7252	10 956.1	10 958.9	−0.025
300.000	44.0422	11 896.2	11 882.6	0.114	300.000	12.2195	10 720.6	10 722.6	−0.019
300.000	35.8493	11 672.3	11 661.2	0.095	300.000	8.5448	10 485.7	10 489.3	−0.035
300.000	28.5495	11 443.4	11 432.1	0.099	300.000	5.3802	10 238.3	10241.4	−0.030
300.000	22.1816	11 209.7	11 197.5	0.109	300.000	2.7652	9 976.3	9 979.6	−0.033
300.000	16.9198	10 978.0	10 968.2	0.089	300.000	1.8022	9 853.6	9 861.3	−0.078
310.000	66.1014	12 174.6	12 179.1	−0.037	310.000	14.8807	10 548.7	10 552.1	−0.032
310.000	57.0760	11 985.6	11 989.9	−0.036	310.000	11.6469	10 341.5	10 345.5	−0.038
310.000	41.6433	11 600.8	11 605.5	−0.041	310.000	8.2980	10 079.9	10 086.1	−0.061
310.000	35.0844	11 404.7	11 408.8	−0.036	310.000	5.8919	9 845.7	9 853.8	−0.082
310.000	28.6621	11 184.6	11 187.8	−0.028	310.000	4.0957	9 629.0	9 637.3	−0.087
310.000	24.0299	11 001.0	11 004.7	−0.034	310.000	2.1673	9 322.1	9 326.0	−0.042
310.000	19.0939	10 775.5	10 779.4	−0.036					
330.000	66.3514	11 838.9	11 830.7	0.069	330.000	4.0360	8 273.4	8 247.8	0.309
330.000	57.9342	11 643.5	11 635.4	0.070	330.000	3.4757	8 020.2	7 994.6	0.320
330.000	49.8890	11 433.0	11 425.0	0.070	330.000	3.0919	7 768.0	7 791.9	−0.308
330.000	42.7054	11 219.3	11 211.4	0.070	330.000	59.6817	11 677.5	11 677.8	−0.003
330.000	36.1854	10 988.7	10 989.6	−0.008	330.000	49.7645	11 424.5	11 421.5	0.026
330.000	30.4841	10 767.7	10 766.0	0.016	330.000	41.4361	11 171.4	11 170.6	0.007
330.000	25.7099	10 551.1	10 549.6	0.014	330.000	34.1157	10 912.9	10 912.1	0.007
330.000	21.5737	10 335.1	10 332.4	0.026	330.000	27.8885	10 654.3	10 652.2	0.019
330.000	18.0465	10 118.2	10 116.7	0.015	330.000	22.1463	10 369.0	10 364.5	0.043
330.000	15.0089	9 899.2	9 898.6	0.006	330.000	17.8569	10 108.2	10 104.0	0.041
330.000	12.5104	9 684.8	9 686.6	−0.018	330.000	14.1189	9 825.4	9 827.1	−0.017
330.000	10.1953	9 446.0	9 450.1	−0.043	330.000	11.0280	9 536.9	9 540.7	−0.040
330.000	8.3086	9 206.7	9 211.9	−0.057	330.000	8.4886	9 231.5	9 237.1	−0.061
330.000	6.9503	8 993.8	8 998.7	−0.055	330.000	6.5.59	8 916.2	8 927.6	−0.128
330.000	5.7103	8 752.5	8 751.3	0.014	330.000	5.0195	8 578.9	8 576.9	0.024
330.000	4.7442	8 508.8	8 496.4	0.146	330.000	3.8756	8 206.3	8 181.1	0.308

Table 6. Continued

T/K	P/MPa	ρ_{exp}/mol·m^{-3}	ρ_{cal}/mol·m^{-3}	% dev	T/K	P/MPa	ρ_{exp}/mol·m^{-3}	ρ_{cal}/mol·m^{-3}	% dev
350.000	67.8479	11 513.0	11 524.5	−0.100	350.000	6.2747	7 377.3	7 476.8	−1.349
350.000	58.7174	11 283.1	11 293.4	−0.091	350.000	5.8635	7 131.1	7 340.3	−2.934
350.000	50.2498	11 037.6	11 047.7	−0.091	350.000	67.9473	11 522.5	11 526.8	−0.037
350.000	43.2639	10 806.6	10 814.4	−0.072	350.000	58.6113	11 289.0	11 290.5	−0.013
350.000	37.2857	10 580.0	10 585.0	−0.047	350.000	50.0793	11 041.0	11 042.4	−0.012
350.000	31.9454	10 345.3	10 348.6	−0.032	350.000	42.5324	10 789.9	10 788.0	0.018
350.000	27.1785	10 100.2	10 102.8	−0.026	350.000	36.3412	10 546.9	10 545.6	0.012
350.000	23.3198	9 868.3	9 870.2	−0.019	350.000	30.7480	10 293.9	10 290.4	0.034
350.000	20.0759	9 638.5	9 641.5	−0.031	350.000	25.8716	10 034.4	10 028.0	0.064
350.000	17.2215	9 400.1	9 404.1	−0.042	350.000	21.8780	9 775.9	9 773.0	0.030
350.000	14.7569	9 154.7	9 158.6	−0.043	350.000	18.4714	9 516.6	9 513.1	0.037
350.000	12.6878	8 905.4	8 908.1	−0.030	350.000	15.6090	9 250.8	9 248.8	0.022
350.000	10.9421	8 649.2	8 647.0	0.026	350.000	13.0007	8 953.1	8 949.4	0.042
350.000	9.4943	8 384.3	8 375.7	0.102	350.000	10.8581	8 641.1	8 632.8	0.096
350.000	8.3961	8 132.8	8 120.2	0.155	350.000	8.9765	8 278.5	8 261.6	0.204
350.000	7.4768	7 868.0	7 863.6	0.056	350.000	7.6945	7 941.8	7 928.1	0.173
350.000	6.7895	7 617.0	7 647.1	−0.395	350.000	6.7931	7 615.6	7 648.3	−0.429

[a] A molecular weight of 120.0200 was used to convert the measured mass densities to the molar densities listed in this table.

Table 7. Parameters of Equation 4 for the Liquid Density of R-125. All b_i Values Not Listed Explicitly Are Equal to Zero

b_3 = 0.085 888 86
b_5 = 0.396 287 939
b_{13} = 0.286 640 635
b_{15} = 0.041 239 614
b_{16} = −0.117 046 818
b_{17} = 0.029 683 657
b_{19} = −0.000 859 869
b_{21} = −9.082 368 767
b_{23} = 3.931 751 612
b_{26} = −1.343 450 734
b_{27} = −0.074 098 578
b_{28} = 0.315 005 759
b_{29} = 0.028 504 544
b_{30} = −0.079 010 346
b_{31} = 0.041 381 424
b_{32} = −0.011 656 952

at temperatures near and below the critical temperature. The excellent agreement of the virial coefficients derived from Burnett measurements in this work and by Boyes and Weber (1995) with those derived by Gillis (1997) from sound speed measurements suggests that the Burnett measurements are not effected significantly by adsorption above the critical temperature. Table 8 contains an analysis which examines the possible effects of adsorption on the isochoric measurements. The column labeled ρ_{400} can be assumed to be free of adsorption because the 400 K isotherm is supercritical and compares well to data reported from other laboratories. The densities in this column come from the isochore pressure at 400 K and the virials derived from Burnett measurements at 400 K. The densities in the two columns labeled ρ_{350} (at 350 K) and ρ_{BW} (at 363 K) have been calculated at the isochore pressures at 350 K and 363.15 K respectively using the virial coefficients at 350 K and 363.15 K respectively and then corrected for volume distortions to provide densities at 400 K. Thus, the entries in these three columns should be identical. While the columns are not exactly identical, they are sufficiently close that any adsorption effects can be assumed to be minor. Had significant adsorption occurred along an isochore upon lowering the temperature, the measured pressure at 350 K would be smaller than that at the same temperature without adsorption. If the density at the measured pressure is calculated using correct parameters from a Burnett isothermal analysis, the calculated density would be significantly smaller than the

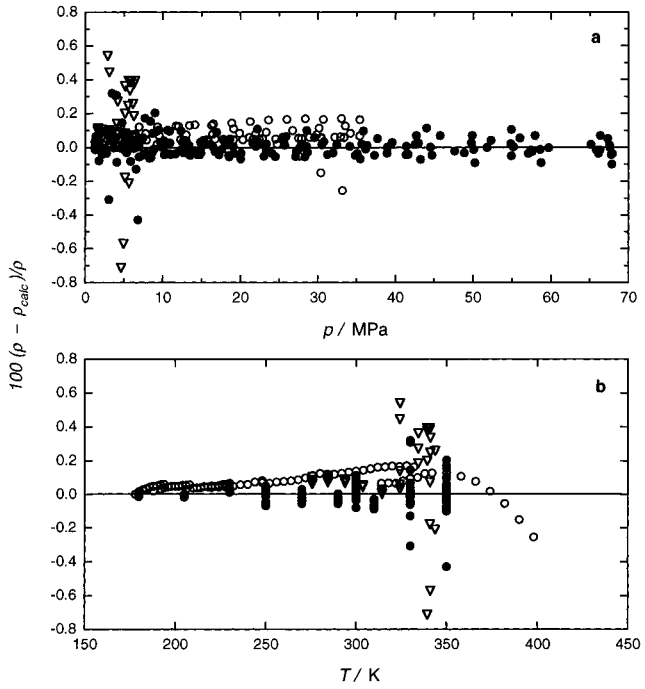

Figure 5. Deviations of the measured compressed liquid densities for R-125 from values calculated using eq 4 and the parameters listed in Table 7. Only the liquid density values measured in this work were used to determine the fitting parameters. The symbols denote: ●, this work; ▽, Defibaugh and Morrison (1992); ○, Magee (1996). Plotted as a function of pressure, a; plotted as a function of temperature, b.

Table 8. Comparison of Burnett Isotherms Using Isochoric Coupling

isochore	ρ_{350}/mol·m^{-3}	ρ_{BW}/mol·m^{-3}	ρ_{400}/mol·m^{-3}	$100(\rho_{BW} - \rho_{350})/\rho_{350})$	$100((\rho_{400} - \rho_{350})/\rho_{350})$
3	1474.8	1475.1	1469.1	0.04	−0.14
4	1165.6	1166.2	1163.9	0.05	−0.15
5	752.8	752.9	751.9	0.02	−0.11
6	533.1	533.3	532.7	0.03	−0.08
7	328.5	328.5	328.4	0.02	−0.02

value calculated at 400 K. The observed discrepancies are slightly larger than expected from an uncertainty analysis for this experiment, and they suggest that the isochoric densities below 350 K probably are accurate to ±0.2%.

Critical Temperature. Critical temperature measurements have been reported by various workers. A summary

Table 9. Critical Constants T_c, P_c, ρ_c, Z_c and Acentric Factor ω for R-125

	T_c/K	P_c/kPa	ρ_c/mol·m^{-3}	Z_c	ω
This work	339.41 ± 0.01	3639.1 ± 0.2	4768.4 ± 7	0.2704 ± 0.0004	0.3038
Shankland *et al.* (1992)	339.4	3631.0	4766.7	0.2699	0.2986
Wilson *et al.* (1992)	339.19	3595.0	4759.6	0.2678	0.3025
Du Pont (1991)	339.4				
Higashi (1994)	339.17	3620.0	4766	0.2694	
Sagawa *et al.* (1994)		3619			
Schmidt and Moldover (1994)	339.33				
Boyes and Weber (1995)		3626.8			
Kuwabara et al. (1995)	339.165		4733		
Tsvetkov *et al.* (1995)		3629			
Ye *et al.* (1995)		3619			
Yata *et al.* (1996)	339.22				
Gillis (1997)	339.45	3630.6			

of critical and reducing parameters for R-125 appears in Table 9. Our critical temperature agrees with those of Shankland *et al.* (1992) (who used a sample of the same high purity, 99.997+ mol %, as ours) and du Pont (1991) within the combined estimated experimental uncertainties. The values reported by Schmidt and Moldover (1994) and Gillis (1997) bracket our value. Our critical temperature is significantly higher than those reported by Wilson *et al.* (1992), Kuwabara *et al.* (1995), Ye *et al.* (1995), and Higachi (1994). The trends in the critical pressures and densities derived from the assigned critical temperatures given in Table 9 are as expected.

Liquid Densities. The two sets of density measurements using the two, different samples agree within ±0.1%. Near the critical region, both sets of results deviate substantially from eq 4. This is a result of the inadequacy of the equation to describe fluid behavior near the critical region and not of inaccuracy in the experimental values. Figure 5a,b presents a comparison of our values to those reported by Defibaugh and Morrison (1992) who report liquid density measurements for R-125 over a temperature range of 275.0 K to 369.0 K with pressures up to 6.3 MPa and with Magee who reports densities between 178 K and 398 K up to 35 MPa. Wilson *et al.* (1992) report a correlation for the liquid density of R-125 based upon measurements over the temperature range of 198.0 K to 448.0 K with pressures up to 10.0 MPa. These results are not included in the figure because they do not report their experimental values, but they do note that the average deviation between their measured liquid densities and those calculated from their fitting equation is ±0.29% with a maximum deviation of ±1.0%.

Conclusions

This paper presents accurate measurements of vapor pressures, liquid densities, vapor densities, and the critical temperature for R-125. Our measurements cover temperatures ranging from 180.0 K to 480.0 K with pressures up to 68 MPa. The vapor pressure measurements are estimated to be accurate within ±0.05%, but our values differ systematically by 0.1 to 0.2% from several other precise data sets over most of the range. Our virial coefficients derived from Burnett measurements agree very well with values derived by other workers from both Burnett and sound speed measurements, and our isochoric vapor densities are internally consistent with the Burnett measurements and in reasonable agreement with other isochoric measurements. The liquid densities have an estimated uncertainty of ±0.1%. Our reported values agree with those of Defibaugh and Morrison (1992) and with Magee (1996) within the combined experimental uncertainties. Our critical temperature agrees well with values reported by several investigators, but it is significantly higher than values reported by several others.

Acknowledgment

The authors acknowledge gratefully Allied Signal and E. I. du Pont Nemours & Company for providing the samples used in this work.

Literature Cited

Baroncini, C.; Giuliani, G.; Latini, G.; Polonara, F.; Camporese, R. Experimental evaluation of thermodynamic properties of refrigerant R125 (CHF_2CF_3). *Sci. Tech. Froid* **1993**, *2*, 207−213.

Boyes, S. J.; Weber, L. A. Vapor pressures and gas-phase (p, ρ, T) values for CF_3CHF_2 (R125). *J. Chem. Thermodyn.* **1995**, *27*, 163−174.

Defibaugh, D.; Morrison, G. Compressed liquid densities and saturation densities of pentafluoroethane (R-125). *Fluid Phase Equilib.* **1992**, *80*, 157−166.

E. I. du Pont Nemours & Company. Private communication, **1991**.

Gillis, K. A. Thermodynamic properties of seven gaseous halogenated hydrocarbons from acoustic measurements: $CHClFCF_3$, CHF_2CF_3, CF_3CH_3, CHF_2CH_3, $CF_3CHFCHF_2$, $CF_3CH_2CF_3$, $CHF_2CF_2CH_2F$. *Int. J. Thermophys.* **1997**, *18*, 73.

Higashi, Y. Critical parameters for HFC134a, HFC32 and HFC125. *Int. J. Refrig.* **1994**, *17*, 524−531.

Holste, J. C.; Hall, K. R.; Iglesias-Silva, G. A. Log-linear plots for data representation. *AIChE J.* **1996**, *42*, 296.

Iglesias-Silva, G. A.; Holste, J. C.; Eubank, P. T.; Marsh, K. N.; Hall, K. R. A vapor pressure equation from extended asymptotic behavior. *AIChE J.* **1987**, *33*, 1550.

Iglesias-Silva, G. A.; Miller, R. C.; Ceballos, A. D.; Hall, K. R.; Holste, J. C. Accurate vapor pressure equation for refrigerants. *J. Fluid Phase Equilib.* **1995**, *111*, 203.

Kuwabara, S.; Aoyama, H.; Sato, H.; Watanabe, K. Vapor-liquid coexistence curves in the critical region and the critical temperatures and densities of difluoromethane and pentafluoroethane. *Chem. Eng. Data* **1995**, *40*, 112−116.

Lau, R. A continuously weighed pycnometer providing densities for carbon dioxide + ethane mixtures between 240 and 350 K at pressures up to 35 MPa. Ph.D. Dissertation, Texas A&M University, College Station, TX, 1986.

Magee, J. W. Isochoric p-ρ-T measurements on difluoromethane (R32) from 142 to 396 K and pentafluoroethane (R125) from 178 to 398 K at pressures to 35 MPa. *Int. J. Thermophys.* **1996**, *17*, 803.

Monluc, Y.; Sagawa, T.; Sato, H; Watanabe, K. Thermodynamic properties of HFC-125. *Symp. Thermophys. Prop.* **1991**, *B101*, 65−68.

Oguchi, K.; Murano, A.; Omata, P.; Yada, N. Experimental study of PVT properties of HFC-125 (CHF_2CF_3). *Int. J. Thermophys.* **1996**, *17*, 55−64.

Sagawa, T.; Sato, H.; Watanabe, K. Thermodynamic properties of HFC-125 based on (p,V,T) measurements. *High Temp.-High Pressures* **1994**, *26*, 193−201.

Shankland, I. R. Allied Signal, private communication, 1992.

Singh, R. Private communication of unpublished data from Allied Signal, 1994.

Stouffer, C. E. Densities of mixtures of carbon dioxide and hydrogen sulfide from 200 to 450 K to 23 MPa by the Burnett-isochoric method. Ph.D. Dissertation, Texas A&M University, College Station, TX, 1992.

Tsvetkov, O. B.; Kletskii, A. V.; Laptev, Yu. A.; Asambaev, A. J.; Zausaev, I. A. Thermal conductivity and PVT measurements of pentafluoroethane (refrigerant HFC-125). *Int. J. Thermophys.* **1995**, *16*, 1185−1192.

Weber L. A.; Silva A. M. Measurements of the vapor pressures of difluoromethane, 1-chloro-1,2,2,2-tetrafluoroethane, and pentafluoroethane. *J. Chem. Eng. Data* **1994**, *39*, 808−812.

Widiatmo, J. V.; Sato, H.; Watanabe, K. Saturated-liquid densities and vapor pressures of 1,1,1-trifluoroethane, difluoromethane, and pentafluoroethane. *J. Chem. Eng. Data* **1994**, *39*, 304−308.

Wilson, L. C.; Wilding, W. V.; Wilson, G. M.; Rowley, R. L.; Felix, V. M.; Chilsom-Carter T. Thermophysical properties of HFC-125. *Fluid Phase Equilib.* **1992**, *80*, 167−177.

Yata, J.; Hori, M.; Kawakatsu, H.; Minamiyama, T. Measurements of refractive index of alternative refrigerants. *Int. J. Thermophys.* **1996**, *17*, 65−74.

Ye, F.; Sato, H.; Watanabe, K. Gas-phase *PVT* properties and vapor pressure of pentafluoroethane (HFC-125) determined according to the Burnett method. *J. Chem. Eng. Data* **1995**, *40*, 148−152.

Yurttas, L. A new isochoric apparatus with applications to *P-V-T* measurements and phase equilibria studies. Ph.D. Dissertation. Texas A&M University, College Station, TX, 1988.

Zhang, H.-L.; Sato, H.; Watanabe, K. Gas phase *PVT* properties for the difluoromethane + pentafluoroethane (R32 + 125)system. *J. Chem. Eng. Data* **1996**, *41*, 1401−1408.

Received for review November 18, 1996. Accepted May 1, 1997.[⊗] The American Society of Heating, Refrigerating and Air Conditioning Engineers has provided the majority of the funding for this work. Additional support has come from the Governor's Energy Management Center-State of Texas Energy Research in Applications (Contract No. 5217), the Center for Energy and Mineral Resources at Texas A&M University and the Texas Engineering Experiment Station.

JE960362F

[⊗] Abstract published in *Advance ACS Abstracts,* June 1, 1997.